Mobility of high-power solitons in saturable nonlinear photonic lattices

Uta Naether,[1,2,*] Rodrigo A. Vicencio,[1,2] and Milutin Stepić[3]

[1]*Departamento de Física, Facultad de Ciencias, Universidad de Chile, Casilla 653, Santiago, Chile*

[2]*Center for Optics and Photonics, Universidad de Concepción, Casilla 4016, Concepción, Chile*

[3]*Vinča Institute of Nuclear Sciences, University of Belgrade, P.O.B. 522, 11001 Belgrade, Serbia*

**Corresponding author: unaether@u.uchile.cl*

Received January 27, 2011; accepted March 5, 2011;
posted March 24, 2011 (Doc. ID 141866); published April 15, 2011

We theoretically study the properties of one-dimensional nonlinear saturable photonic lattices exhibiting multiple mobility windows for stationary solutions. The effective energy barrier decreases to a minimum in those power regions where a new intermediate stationary solution appears. As an application, we investigate the dynamics of high-power Gaussian-like beams finding several regions where the light transport is enhanced. © 2011 Optical Society of America

OCIS codes: 190.0190, 190.5330, 190.6135, 230.4320.

For more than a decade, nonlinear waveguide arrays (WAs) have become an excellent experimental scenario to study the phenomenology appearing in periodic and nonperiodic nonlinear dynamical systems [1–3]. Different geometries, dimensions, and nonlinearities have been studied showing interesting and very different phenomenologies compared to continuous systems. For WAs with Kerr nonlinearity, a coupled mode approach leads to a discrete nonlinear Schrödinger (DNLS) equation. For photorefractive media with saturable nonlinearity, the corresponding model is an s-DNLS [4,5].

Mobility of localized solutions in nonlinear cubic WAs is well known. As long as the power stays low, the energy barrier imposed by the discreteness and the nonlinearity {usually called Peierls–Nabarro (PN) potential [6]}will stay small and solutions will move across the lattice by just giving them a judicious kick [7,8]. For larger powers, the energy barrier grows, and mobility is not possible anymore. However, for saturable systems, there are several regions of power where the energy difference between the two fundamental localized solutions—the one centered at one site (odd mode) and the one centered between two sites (even mode)—vanishes for different power values [4,5]. Close to these points, there are regions of stability exchange between the even and odd solutions. Since those regions exhibit bistability, the appearance of an intermediate asymmetric and unstable solution is inevitable, as it was shown in [9,10] for two-dimensional systems. Therefore, in this case, the *effective* energy barrier will strongly depend on the intermediate solutions (ISs). For saturable one-dimensional (1D) systems, this crucial issue has not been clearly identified yet. We believe this element could be one of the keys to experimentally observe, to the best of our knowledge for the first time, good soliton mobility in 1D nonlinear saturable photonic lattices.

It was shown in [4,5] that the PN barrier becomes minimal exactly at the points where the fundamental solution's energies coincide. Contrary to what is expected, the fundamental solutions remain immobile in these points. We demonstrate that, in order to achieve a good mobility, it is necessary to increase the amount of power up to the bifurcation point where the IS disappears. A constraint method [10–12] is used to identify the ISs and describe a pseudopotential landscape among all stationary modes. By using the system properties, we found recurrent resonant behavior in power for Gaussian-like shaped pulses showing enhanced mobility.

In a 1D system, the s-DNLS is given by

$$i\frac{du_n}{dz} + (u_{n+1} + u_{n-1}) - \gamma\frac{u_n}{1+|u_n|^2} = 0, \qquad (1)$$

where u_n represents the light amplitude at site n, γ the strength of the nonlinearity with respect to the coupling coefficient, and z a normalized propagation distance along the waveguides. In order to understand the main phenomenology of these lattices, we first look for stationary solutions of the form $u_n(z) = u_n \exp(i\lambda z)$, where $u_n \in R$, and λ is the propagation constant or frequency. Small-amplitude plane waves define the band $\lambda \in [-2-\gamma, 2-\gamma]$, while high-amplitude plane waves define a second band $\lambda \in [-2, 2]$. Therefore, in-phase stationary localized solutions are limited to exist in the region $\lambda \in [2-\gamma, 2]$, bifurcating from the fundamental modes of those bands [9]. Model (1) has two dynamically conserved quantities: the Hamiltonian $H = -[\sum_n (u_{n+1}u_n^* + u_n u_{n+1}^*) - \gamma \log(1+|u_n|^2)]$ and the optical power $P = \sum_n |u_n|^2$.

In the following, we discuss these properties for $\gamma = 10$ (focusing nonlinearity). A different γ will produce different curves, but the main saturable phenomenology will be preserved. Localized solutions are computed by using a standard Newton–Raphson method. Figure 1 shows a power versus frequency diagram for both fundamental modes—the odd and the even solutions—including the IS. As expected, the IS corresponds to a nonsymmetric profile connecting the two fundamental modes (see Fig. 1 inset). The two fundamental solutions cross each other—repeatedly—as P increases. In regions where $|P_{\text{odd}} - P_{\text{even}}|$ is large, a family of IS appears. It is remarkable that all the ISs of the first family have $\lambda = 0$ and connect both (even and odd) modes for this value. In such a situation, the stationary solutions of Eq. (1) coincide with the ones of the integrable Ablowitz–Ladik equation [13], which has an analytic mobile solution. However, in the physical

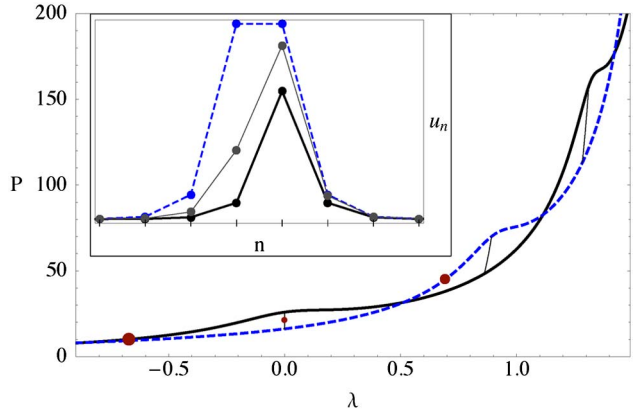

Fig. 1. (Color online) P versus λ for odd solutions, even solutions, and ISs in full, dashed, and thin curves, respectively. Inset: profiles corresponding to filled circles.

s-DNLS model, it is not expected to find radiationless travelling solutions, since mobile modes need to have the same power and not the same frequency. We perform a standard linear stability analysis [14] by computing the largest imaginary part ("g") of the eigenvalue spectrum. Figure 2(a) shows our results where $g = 0$ implies stable solutions and $g > 0$ unstable ones. For all regions where the fundamental solutions are simultaneously stable (three regions in this plot), the unstable IS appears. In these regions there are points where the energy of both fundamental solutions is exactly the same [see inset in Fig. 2(a) for the first bistable region ($P \sim 20$)]. However, the effective energy barrier is not zero if the IS is considered as well. In Fig. 2(b) we plot $\Delta H_0 \equiv |H_{\text{odd}} - H_{\text{even}}|$ and $\Delta H \equiv |H_{\max} - H_{\min}|$ versus power.

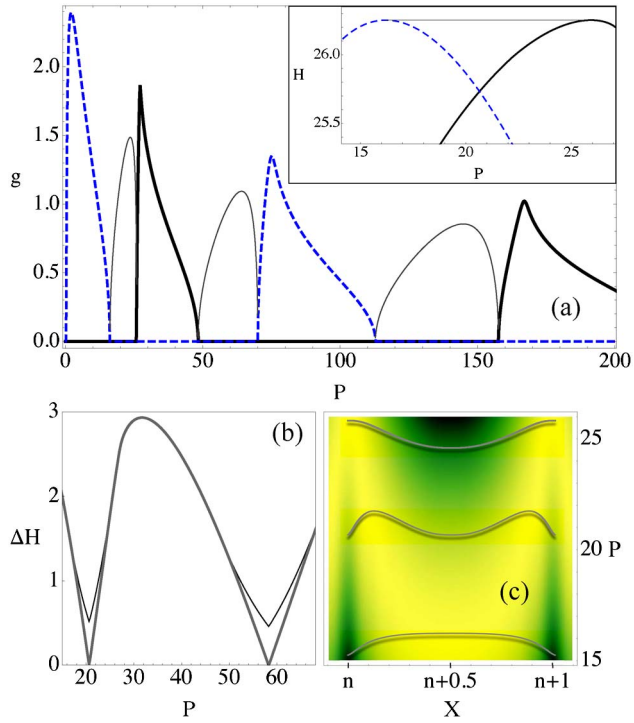

Fig. 2. (Color online) (a) g versus P for odd solutions, even solutions, and ISs in full, dashed, and thin curves, respectively. Inset: H versus P. (b) ΔH_0 (thick curve) and ΔH (thin curve) versus P. (c) Energy surface where light (dark) color denotes a high (low) H value.

For the first two "bistable" regions, we clearly see that ΔH_0 goes to zero as it was previously predicted in [4,5]. However, there is always a nonzero barrier (ΔH) for the solution, which can be very small but it is—strictly speaking—nonzero. A first guess could be that the most favorable region for mobility would be the one where ΔH is a minimum. However, this is not the case for stationary solutions. If we kick an odd or even mode, we are putting in motion an immobile-defined solution; therefore, there is always radiation from tails. As a consequence, the power of the moving solution is lower than the initial one. So, if we initially take the solution where ΔH is a minimum (P_m), the effective barrier will increase [see Fig. 2(b)]. A better option would be the one where $P > P_m$ where, due to radiation, the power and the effective barrier decrease. Now, in order to go deeper in the understanding of the dynamics of 1D saturable WAs, we construct an energy landscape. By defining the center of mass $X \equiv \sum_n n|u_n|^2/P$ and using a constraint method [10–12], we compute H versus X and P. Figure 2(c) shows our computations around the first bistable region. In this plot, $X = n$ and $n + 1$ correspond to odd modes while $X = n + 0.5$ corresponds to even ones. For low power, the potential is cubiclike in the sense that the odd mode is stable while the even one is unstable (lower curve for $P = 15$). By increasing the power, both fundamental solutions are simultaneously stable, because they are both a local minimum in this potential. Consequently, a maximum in-between appears, the unstable IS (middle curve for $P = 20.5$ where $\Delta H_0 \approx 0$). Then, by further increasing the power, the odd solution transforms into an unstable maximum while the even one becomes the only minimum of this potential (upper curve for $P = 26$). The IS originates when the even mode stabilizes; then, it changes its center of mass to an odd mode (symmetrically to the right and to the left due to the system symmetry). Finally, the IS disappears when the odd mode destabilizes.

To the best of our knowledge, mobility in this kind of system was never predicted for a more realistic experimental input condition like Gaussian input profiles. Previous simulations, starting from stationary solutions, observed good mobility [4,5,9,10,13]. However, saturable solutions are not well localized in the power-exchange regions, and, furthermore, by increasing the power, they become broader. Therefore, in an experiment, dynamics will be strongly determined by the power and shape of the chosen beam profile. We took as an input beam a five-site-wide Gaussian-like profile: $u_n(0) = A \exp[-\alpha(n-n_c)^2] \exp[ik(n-n_c)]$ for $n = n_c, n_c \pm 1, n_c \pm 2$, and $u_n(0) = 0$ otherwise. The kick k is proportional to the experimental angle, and it does not alter the power but adds a small amount of effective kinetic energy. With this initial condition, we numerically integrate model (1) from $z = 0$ to $z = z_f$ and measure the center of mass at the lattice output: $X_f \equiv X(z_f)$. Figure 3(a) shows our results for different input power (P). For very low power ($P \sim 0$), the system is linear and mobility decreases as system becomes nonlinear up to $P \approx 50$, when the saturable system behaves as a cubic one [see Fig. 3(b)]. Then, by further increasing the power, solutions start to move. When the power is increased, fundamental solutions are geometrically similar and differences in the Hamiltonian are very

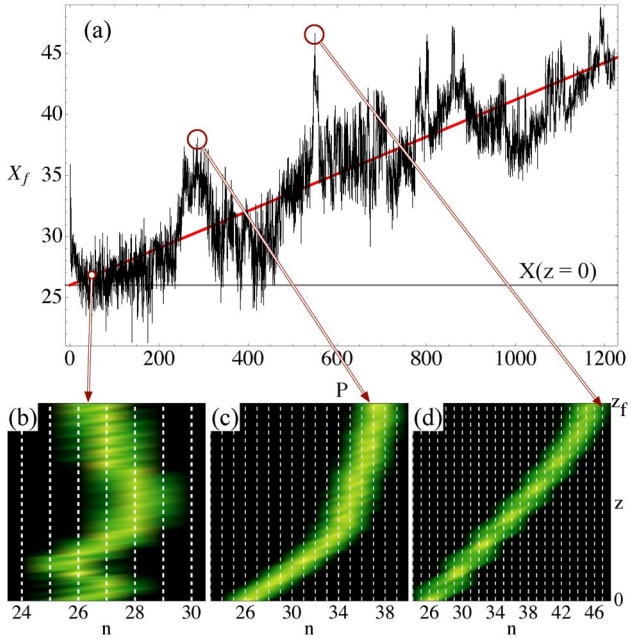

Fig. 3. (Color online) (a) Output X_f versus input P. (b), (c), (d) Dynamical examples for $P = 54$, 300, and 550, respectively. $\gamma = 10$, $n_c = 26$, $k = 0.3$, $\alpha = 1/3$, $z_f = 50$.

small; therefore, the profile is allowed to move with $k \neq 0$, as it is observed in the average tendency of the curve [diagonal straight line in Fig. 3(a)]. However, some "resonant" dynamics are found for different levels of power. There are different regions where mobility is enhanced as shown in Figs. 3(c) and 3(d), with almost undamped motion. It is plausible to assume that this behavior corresponds to a manifestation of the continuously repeating bistable regions discussed for stationary solutions. Therefore, for even higher powers, there should be good mobility, in principle without limitations. The mobility windows for Gaussian pulses do not coincide with the mobility regions for stationary solutions, since a Gaussian pulse will always have a higher cost in power loss due to radiation and due to its shape (Gaussian profiles do not match in shape and power with any fixed stationary solution, which implies different levels of power to observe similar dynamics). But, nevertheless, the recurrent appearance of enhanced mobility for certain powers shows an excellent phenomenological agreement between Gaussian and stationary profiles.

To conclude, we have shown that, in nonlinear saturable 1D photonic lattices, there are several regions of bistability where stationary solutions possess a small but nonzero energy barrier. The effective energy barrier among all stationary localized solutions was constructed, allowing us to get a deeper understanding of discrete saturable nonlinear systems. By using these properties with a more realistic input condition, we were able to observe very good mobility and also to find different regions of resonant response where the mobility is enhanced. We hope that these findings will motivate experimentalists to explore this direction of high-power mobility, which is currently a drawback for the implementation of nonlinear WAs in realistic all-optical operations in different power regimes.

The authors thank Magnus Johansson for discussions and acknowledge financial support from Fondo Nacional de Desarollo Científico y Tecnológico (FONDECYT) grant 1070897, Programa de Financiamiento Basal de Comisión Nacional de Investigación Científica y Tecnológica (CONICYT) (FB0824/2008), CONICYT fellowship, and the Ministry of Science and Technological Development of Republic Serbia (project III45010).

References

1. F. Lederer, G. I. Stegeman, D. N. Christodoulides, G. Assanto, M. Segev, and Y. Silberberg, Phys. Rep. **463**, 1 (2008).
2. S. Flach and A. V. Gorbach, Phys. Rep. **467**, 1 (2008).
3. Y. V. Kartashov, V. A. Vysloukh, and L. Torner, Prog. Opt. **52**, 63 (2009).
4. M. Stepić, D. Kip, L. Hadžievski, and A. Maluckov, Phys. Rev. E **69**, 066618 (2004).
5. Lj. Hadžievski, A. Maluckov, M. Stepić, and D. Kip, Phys. Rev. Lett. **93**, 033901 (2004).
6. Y. S. Kivshar and D. K. Campbell, Phys. Rev. E **48**, 3077 (1993).
7. U. Peschel, R. Morandotti, J. M. Arnold, J. S. Aitchison, H. S. Eisenberg, Y. Silberberg, T. Pertsch, and F. Lederer, J. Opt. Soc. Am. B **19**, 2637 (2002).
8. R. A. Vicencio, M. I. Molina, and Y. S. Kivshar, Opt. Lett. **28**, 1942 (2003).
9. R. A. Vicencio and M. Johansson, Phys. Rev. E **73**, 046602 (2006).
10. U. Naether, R. A. Vicencio, and M. Johansson, Phys. Rev. E **83**, 036601 (2011).
11. M. I. Molina, R. A. Vicencio, and Y. S. Kivshar, Opt. Lett. **31**, 1693 (2006).
12. C. R. Rosberg, D. N. Neshev, W. Krolikowski, A. Mitchell, R. A. Vicencio, M. I. Molina, and Y. S. Kivshar, Phys. Rev. Lett. **97**, 083901 (2006).
13. T. R. O. Melvin, A. R. Champneys, P. G. Kevrekidis, and J. Cuevas, Phys. Rev. Lett. **97**, 124101 (2006).
14. A. Khare, K. Ø. Rasmussen, M. R. Samuelsen, and A. Saxena, J. Phys. A **38**, 807 (2005).